

## LUMINESCENT PROPERTIES OF ZnO MICROSTRUCTURES GROWN ON Au/Si SUBSTRATE

R. GARCIA-GUTIERREZ, P. HORTA-FRAIJO, A. RAMOS-CARRAZCO\*,  
D. BERMAN-MENDOZA

*Departamento de Investigación en Física de la Universidad de Sonora,  
Hermosillo, Sonora, C.P. 83000, México*

ZnO microstructures have been grown on gold coated silicon substrate at 600°C by chemical vapor deposition. A rough surface showing two different crystal morphologies was observed in the scanning electron microscope. The characteristic crystallographic plane (0002) of the zinc oxide was identified using the XRD pattern. To compare the luminescence properties of the deposit, an air annealing was performed at 100°C, 300°C and 500°C. The trapping levels produced on this oxide were studied by the thermoluminescence after beta radiation. The room-temperature photoluminescence spectra of the samples show two peaks related with the edge band emission and the green band typical of the ZnO. In contrast, the room-temperature cathodoluminescence spectra present a dominant edge band emission.

(Received August 3, 2016; Accepted September 23, 2016)

*Keywords:* Zinc oxide; Luminescence; Chemical vapor deposition; Gold coated silicon

### 1. Introduction

Zinc oxide (ZnO) is a versatile material that has attracted interest because of outstanding electrical, optical, piezoelectric and pyroelectric properties. ZnO semiconductor is widely used in varistors, ultraviolet detectors, emission devices, thin film transistors and surface acoustic wave systems. [1-4]. Recently, the optoelectronic properties of ZnO are considered attractive due to its wide band gap of 3.37 eV, n-type background concentration, exciton binding energy of 60 meV and high transparency of 80% in the visible region [5-6]. Based on the morphological features, the characterization of ZnO has been widely studied for promising technologies as ultraviolet light emitting diodes, laser diodes and sensors [7-9]. Mostly, the microstructures derived of this semiconductor such as tubes, wires, belts, helixes and rods have gained the attention of researchers. The research of the semiconductor based devices is directed towards the control of composition, transparency, conductivity and crystal structure. Recently, the high quality of ZnO has been an important challenge for the manufacture of optoelectronic devices [10-11].

Many techniques can be applied to synthesize zinc oxide such as microwave plasma deposition [12], sputtering [13], hydrothermal synthesis [14] and electrochemical deposition [15-17]. The chemical vapor deposition is convenient for the growth of a wide range of microstructures such as wires, belts and rings [18]. In this work, the growth of ZnO microstructures on Au/Si substrate by chemical vapor deposition (CVD) is reported. By means of scanning electron microscope (SEM), the presence of ZnO microstructures grown on Au/Si substrate was demonstrated. The wurtzite structure of this oxide was identified by X-ray diffraction (XRD). The thermoluminescence (TL) response of the zinc oxide samples was characterized to identify the different trapping levels. The optical emission of the oxide was characterized by means of cathodoluminescence (CL) and photoluminescence (PL).

---

\* Corresponding author: antonio.ramos@unison.mx

## 2. Experimental

Figure 1 shows the schematic diagram of the chemical vapor deposition system used for the growth of ZnO microstructures. The synthesis of the semiconductor was carried out in a three-zone flow-type quartz reactor. This CVD reactor consists of a quartz tube of 63 mm of diameter placed inside of one horizontal furnace. To introduce the high purity gases of oxygen ( $O_2$ ) and argon (Ar), two concentric quartz tubes of 19 mm of diameter were positioned. The starting reagents used were high-purity Zn (99.99%), argon and oxygen gases. The vapor of zinc takes form in the first zone while oxidation occurs on the substrate (Au/Si) in the second zone. The deposits were performed on standard 50 mm silicon wafers with a surface resistivity of  $10 \Omega$ . Previous to deposition, each substrate was cleaned by a chemical solution and covered with an Au thin layer ( $\sim 50$  nm) by sputtering.

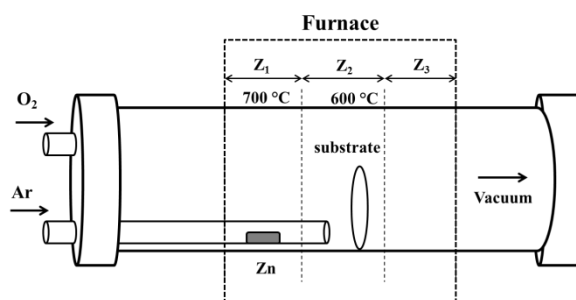


Fig. 1. Schematic diagram of the horizontal reactor used for the growth of ZnO microstructures by chemical vapor deposition.

The procedure for the growth of ZnO microstructures is presented by the following steps. Once the boats containing the substrate (Au/Si) and metallic Zn are placed inside the quartz tube, a mechanical pump provides a vacuum in the chamber (1.3 Pa). In order to decrease the impurities inside of the CVD reactor, an argon flux is provided and purged several times. A thermal treatment of the substrate was completed at 900 °C during one hour. Then, the temperature of zone 2 is decreased to 600 °C and an oxygen flux of 200 sccm is provided. An argon flux of 200 sccm is introduced to carry the Zn vaporized towards the substrate zone. The pressure of the reactor was maintained at 2 kPa and the reaction time was 15 minutes. Finally, the system is cooled down to room temperature and the sample is stored for further characterization.

The SEM images were taken in a scanning electron microscope model JEOL JSM 6300 using an acceleration voltage of 15 kV, beam current of 300 pA, slit width of 0.12 mm and a spot size of  $2 \times 1.5 \mu\text{m}$ . The X-ray diffraction patterns were recorded by a powder diffractometer model X'pert Philips in a range of 20 to 70 degrees ( $2\theta$ ) at room temperature. The thermoluminescence characterization was performed using a RISØ TL /OSL-DA-20 system provided with a  $^{90}\text{Sr}$ - $^{90}\text{Y}$  beta radiation source with a dose rate of  $0.1 \text{ Gys}^{-1}$ . The TL measurements were obtained from 30 °C to 400 °C at a heating rate of  $1 \text{ Cs}^{-1}$  and a dose rate of  $0.1 \text{ Gys}^{-1}$ . The TL curves were detected using a photomultiplier tube EMI 9235QB with a quantum efficiency in the wavelength range between 160 nm and 630 nm. The PL characterization was performed using an HeCd laser with a wavelength of 325 nanometers and recorded using an OCEAN VIEW spectrometer REDTIDE 650. For the CL spectrum, the emissions were obtained using a JEOL JIB-5400 scanning electron microscope with an acceleration voltage of 15 kV as the excitation source. Both luminescence methods were realized under room temperature conditions.

## 3. Results and discussion

Fig. 2 presents SEM images of the surface morphology of the ZnO deposit grown on the Au/Si substrate. Two types of crystals can be identified from the plane view in the SEM

micrograph shown in Figure 2-(A). The first type has the form of rods with a length and diameter in the micrometer and nanometer scales, respectively. The second type of crystals were notably large structures which shows an irregular polyhedral behavior. Also, hexagonal microstructures with a diameter of 5  $\mu\text{m}$  were observed in the surface, as is presented in Figure 2-(B). According to the cross-section SEM image, the deposition of ZnO grown on the Au/Si wafer exhibits an approximate thickness of 15  $\mu\text{m}$ , as is shown in Figure 2-(C). The use of a gold layer on semiconductor substrates has been an important issue for the growth of ZnO microstructures. After annealing, the metallic layer creates Au drops that work as nucleation sites, as was previously reported [19]. However, the lack of control in the size of the drops tends to undistributed nucleation sites which produces different growth regimes. Figure 2-(D) shows energy dispersive X-ray spectroscopy (EDS) analysis of one ZnO hexagonal microcrystal. The presence of carbon was observed in the EDS spectrum and can be related with contamination with the environment. No other metals or impurities were found in the surface.

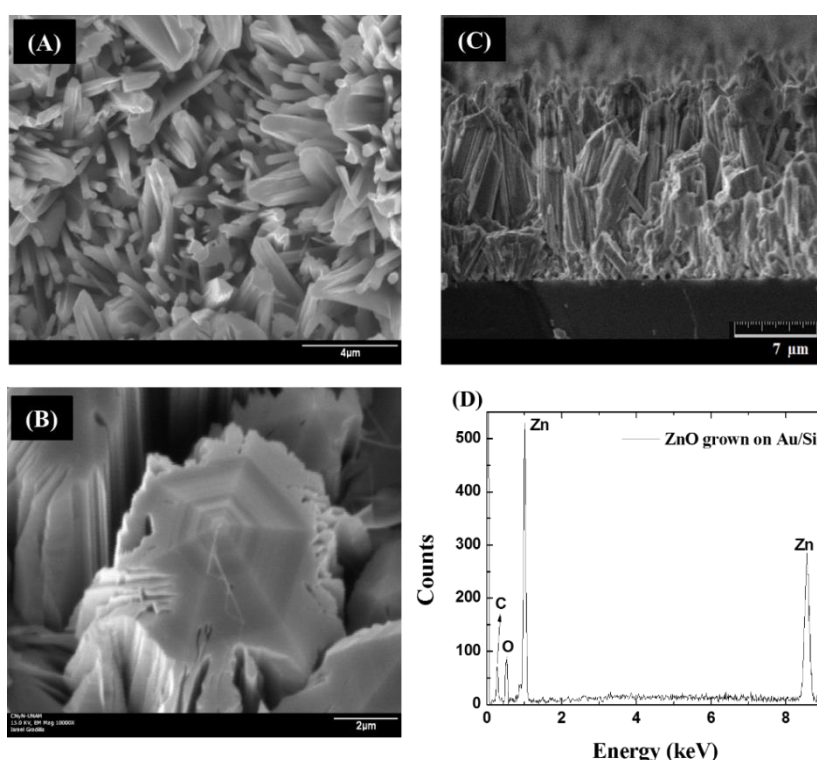


Fig. 2. SEM images of the surface (A-B) and cross section of (C) ZnO microstructures grown Au/Si substrate. (D) Energy dispersive X-ray spectroscopy (EDS) spectra of ZnO microcrystal.

To determine the crystalline structure, the X-ray patterns were measured for ZnO microstructures, as shown in Fig. 3. Using the strongest XRD peak and the 2theta position, the wurtzite phase was identified according to the PDF card 00-36-1451. The characteristic diffraction peaks associated to the presence of pure metals or other oxides were not observed. Only the diffraction peak associated with the silicon substrate was found. ZnO present one preferential XRD peak corresponding to the basal plane (0002) of the hexagonal wurtzite with a slight difference of the 2theta position. Therefore, zinc oxide rods share crystallographic features with the larger formations in the deposit.

Fig 4 show the TL glow curves of ZnO microstructures after been exposed to  $\beta$  radiation doses of 1 Gy, 25 Gy, 75 Gy and 100 Gy. In order to compare the defect related emissions, a thermal treatment of 100  $^{\circ}\text{C}$ , 300  $^{\circ}\text{C}$  and 500  $^{\circ}\text{C}$  were applied to samples. The curves of the ZnO samples exhibit a low-temperature peak centered at 100  $^{\circ}\text{C}$  and a high-temperature peak located beyond the 400  $^{\circ}\text{C}$ .

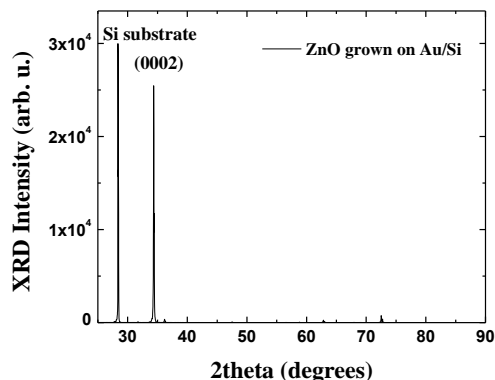


Fig. 3. XRD  $2\theta$  scan diagrams of ZnO grown on Au/Si substrate by chemical vapor deposition. The pattern shows the presence of the (0002) preferred hexagonal wurtzite.

The shape of the TL response is associated to shallow and deep trapping levels of the charge carriers. Also, the luminescence response is consistent as function of the increment of the  $\beta$  doses. It should be mentioned that the spectral emission of these TL curves is not presented. However, the detection efficiency of the sensor has a wavelength range between 160 nm and 630 nm which is congruent to the typical emission range of this oxide. The increment of the TL signal was only significantly affected under air annealing at 500 °C, as is shown in Figure 4-(C). This result can be associated with the rich-oxygen surface obtained in the ZnO microstructures.

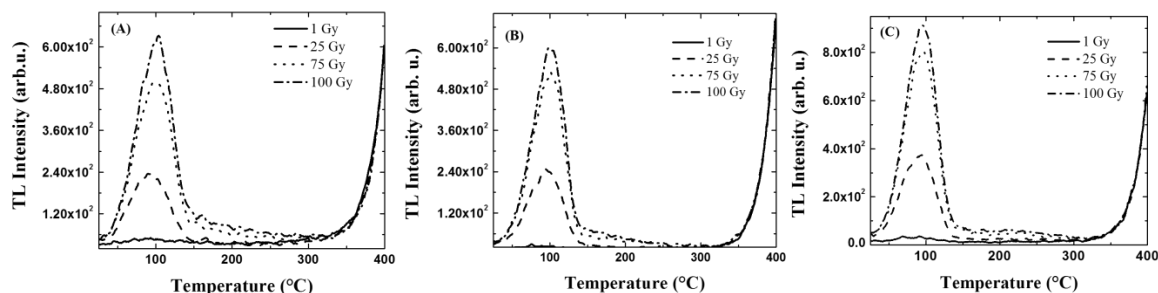


Fig 4. TL glow curves of ZnO microstructures after exposed to 1 Gy, 25 Gy, 75 Gy and 100 Gy of beta radiation. The TL response was measured after an annealing of the samples at (A) 100°C, (B) 300°C and (C) 500°C.

Fig. 5 presents the room-temperature PL spectra of the ZnO microstructures grown on Au/Si substrate after thermal treatment at 100°C, 300°C and 500 °C. Under 325 nm excitation, the spectra are dominated by a short-wavelength band at 3.2 eV and a broad long-wavelength band centered at 2.24 eV. These transitions are related to the edge luminescence and the green luminescence in the ZnO. Based on earlier data on the optical emission of this oxide [20], the band-edge emission is attributed to free excitons while the green band is associated to oxygen deficiency. Also, the annealing of the microstructures indicates that the green band present a strong dependence on this thermal treatment. The difference in PL intensity is produced by the increasing composition of native defects and impurities due to the air annealing.

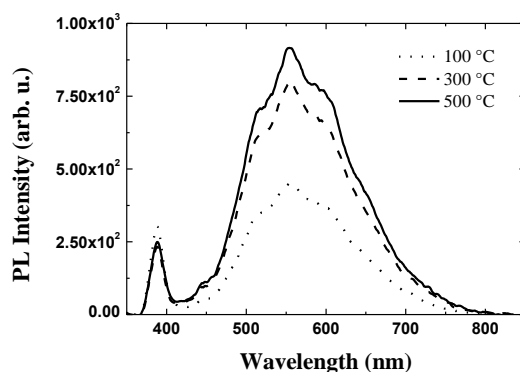


Fig. 5. Room-temperature PL spectra of ZnO microstructures under excitation at 325 nm; Annealing of the samples at (A) 100°C, (B) 300°C and (C) 500°C.

Fig. 6 shows room-temperature CL spectra of the ZnO semiconductor grown on Au/Si by the CVD technique. Also the comparison of optical responses after air annealing at 100°C, 300°C and 500°C are presented. At room temperature, the strongest emission is peaked at 3.2 eV that arises from the band-edge emission of the ZnO. The green band located at 2.3 eV is also present in the CL spectra in all samples.

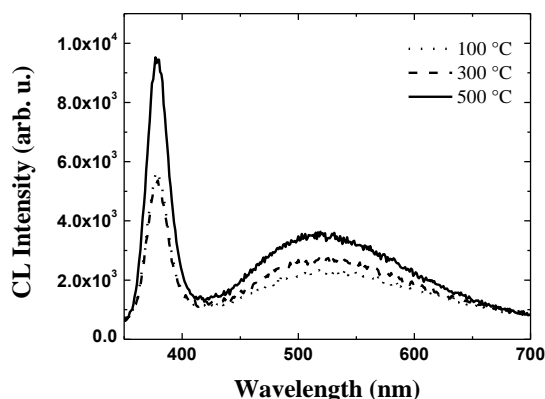


Fig. 6. Room-temperature CL spectra of ZnO microstructures under excitation with 15 kV; Annealing of the samples at (A) 100°C, (B) 300°C and (C) 500°C.

In comparison with the PL results, the CL luminescence of ZnO shows a different behavior. The UV emission dominates the optical response and enhances with the annealing at 500°C. On the other hand, the green emission relatively remains the same after the thermal treatment. Given that the relative intensities of the PL and CL measurements show a radical difference, each spectrum should be analyzed. For the PL spectrum, the characterization technique obtains a superficial emission of the material. According to previous reports, the penetration depth of ultraviolet light in the ZnO approaches 40 nm [21]. Therefore, absorption of light only provides a surface result for this semiconductor by means of PL. Recalling the TL discussion, the surface may present an enrichment of oxygen in the ZnO. Therefore, the optical emission after air annealing can be associated with increased oxygen vacancies and donor-acceptor pairs with oxygen vacancies on the surface. In comparison, the excitation source of the CL method presents a penetration depth greater than UV light. The beam of high-energy electrons can penetrate into materials from 0.04 to 2 micrometers by varying the acceleration voltage [22]. Therefore, the CL spectrum obtains data from ZnO bulk and is not limited to a surface characterization.

#### 4. Conclusion

The luminescence response of the ZnO grown on Au/Si by means of CVD is presented. The nucleation of microstructures was achieved using the metallic layer and a thermal treatment of the substrate. Two different morphologies were found on the surface of the oxide which involve different regimes of growth. The wurtzite structure was identified using the X-ray pattern of the ZnO synthesized on the surface of the Au nucleation sites. The characteristic trapping levels produced on the semiconductor were studied and identified by the TL glow curves. At least two transitions were classified from the TL signal as shallow and deep traps. The edge-band emission and the green band was obtained by means of PL and CL techniques. The interaction of the excitation source of each luminescence method was exposed and a different behavior of the optical properties of the ZnO was obtained.

#### Acknowledgements

The authors gratefully acknowledge the use of facilities within the Universidad de Sonora (UNISON). This research has been partially supported by CONACyT México, project number 102671.

#### References

- [1] D. D. Wang, J. H. Yang, L. L. Yang, Y. J. Zhang, J. H. Lang, M. Gao, *Crys. Res. Technol.* **43**, 1041 (2008).
- [2] Z. L. Wang, *Mater. Today* **7**, 26 (2004).
- [3] P. Nunes, E. Fortunato, P. Tonello, F. Barz-Fernandez, P. Vilarinho, R. Martins, *Vacuum* **64**, 281 (2002).
- [4] X. Ma, Z. Wang, *Mat. Sci. Semicond. Process.* **15**, 227 (2012).
- [5] W. Liu, S. Zhao, Wei Sun, Y. Zhou, K. Jin, H. Lü, M. He, G. Yang, *Physica B* **404**, 1550 (2009).
- [6] M. Arnold, P. Avouris, Z. W. Pan, Z. L. Wang, *J. Phys. Chem. B* **107**, 659 (2003).
- [7] X. D. Wang, C. J. Summers, Z. L. Wang, *Nano Lett.* **4**, 423 (2004).
- [8] L. Dong, J. Jiao, D. W. Tuggle, J. M. Patty, S. A. Ellif, M. Coulter, *Appl. Phys. Lett.* **82**, 1097 (2003).
- [9] Z. L. Wang, J. H. Song, *Science* **312**, 242 (2006).
- [10] E. Ziegler, A. Heinrich, H. Oppermann, and G. Stover, *phys. stat. sol. (a)* **66**, 636 (1981).
- [11] M. J. Brett and R. R. Parsons, *J. of Mater. Sci.* **22**, 3611 (1987).
- [12] T. C. Lin, C. Y. Wang, L. H. Chan, D. Q. Hsiao, H. C. Shih, *J. Vac. Sci. Technol. B* **24**, 1318 (2006).
- [13] S. H. Ko, D. Lee, H. W. Kang, K. H. Nam, J. Y. Yeo, S. J. Hong, C. P. Grigoropoulos, and H. J. Sung, *Nano Lett.* **11**, 666 (2011).
- [14] Z. Dong, B. Han, S. Qian, and D. Chen, *J. Nanomater.* **2012**, 251276 (2012).
- [15] J. Cembrero, A. Elmanouni, B. Hartiti, M. Mollar, and B. Mari, *Thin Solid Films* **451**, 198 (2004).
- [16] W. I. Park, G. C. Yi, M. Kim, S. J. Pennycook, *Adv. Mater.* **14**, 1841 (2002).
- [17] B. Mari, M. Mollar, A. Mechkour, B. Hartiti, M. Perales, and J. Cembrero, *Microelectron. J.* **35**, 79 (2004).
- [18] M. Fahoume, O. Maghfoul, M. Aggour, B. Hartiti, F. Chraïbi, and A. Ennaoui, *Sol. Energ. Mat. Sol. C.* **82**, 85 (2004).
- [19] R. Garcia-Gutierrez, M. Barboza-Flores, D. Berman-Mendoza, R. Rangel-Segura, O. E. Contreras-Lopez, *Adv. Mater. Sci. Eng.* 872597, 2012.
- [20] A. N. Gruzintev, E. E. Yakimov, *Inorganic Materials* **41**, 725 (2005).
- [21] L. Luo, Y. Zhang, S. S. Mao, L. Lin, *Sensors and Actuators A* **127**, 201 (2006)
- [22] N. Bano, I. Hussain, O. Nur, M. Willander, Q. Wahab, A. Henry, H. S. Kwack, D. Le Si Dang, *J. Lumin.* **130**, 963 (2010).